International Journal of Multiphase Flow 85 (2016) 76–85

Contents lists available at ScienceDirect

International Journal of Multiphase Flow

journal homepage: www.elsevier.com/locate/ijmultiphaseflow

Elongated bubble shape in inclined air-water slug flow

E. Roitberg[1], D. Barnea, L. Shemer*

School of Mechanical Engineering, Tel-Aviv University, Israel

ARTICLE INFO

Article history:
Received 21 December 2015
Revised 29 March 2016
Accepted 21 May 2016
Available online 26 May 2016

ABSTRACT

The shape of elongated bubbles in upward inclined air-water slug flow was studied experimentally by quantitative measurements of the cross sectional distribution of the phases within the pipe, using a wire mesh sensor. Ensemble-averaged shapes of elongated bubbles were determined for a wide range of gas and liquid flow rates, as well as for different pipe inclination angles. The elongated bubble nose can be characterized by an annular domain where liquid is present above the gas. The effect of gas and liquid flow rates, as well as of the pipe inclination angle on the bubble shape (front and tail) is studied. A simplified theoretical model is proposed to determine the bubble front shape. The model predictions compare favorably with the experimental results.

1. Introduction

Gas-liquid slug flow is characterized by intermittency and irregularity. Each slug unit is composed of a liquid slug zone that fills the whole cross-section of the pipe and may be aerated by dispersed bubbles, and an elongated bubble zone. In horizontal and inclined pipes, the elongated bubbles overlay a non-uniform stratified liquid layer flowing along the bottom of the pipe. In vertical flow, most of the gas is located in large bullet-shaped (Taylor) bubbles, which span most of the pipe's cross-section. The liquid confined between the elongated bubble and the pipe wall flows around the bubble as a thin film.

Mechanistic models that are capable of simulating pressure drop and flow behavior with relatively high degree of confidence were introduced by Dukler and Hubbard (1975) and Nicholson et al. (1978) for horizontal flow, and Fernandes et al. (1983), Orell and Rembrandt (1986) and Sylvester (1987) for vertical flow. More comprehensive approaches to slug flow modelling for the whole range of pipe inclinations were introduced by Taitel and Barnea (1990) and Fabre and Line (1992).

The elongated bubble is characterized by three regions: the bubble front, or nose, the bubble tail, and its body. The body of the elongated bubble can be reasonably approximated as a one-dimensional steady-state film flow (Dukler and Hubbard 1975, Kokal and Stanislav 1989, Taitel and Barnea 1990, Andreussi et al. 1993, Cook and Behnia, 2000 and Fagundes Netto et al. 1999).

Benjamin (1968) employed the inviscid theory to calculate the bubble nose shape and the drift velocity of an isolated bubble in a horizontal pipe. Fagundes Netto et al. (1999) used the model by Benjamin to estimate the nose shape and matched it with the film model in the body of the elongated bubble. Taitel and Barnea (1990) suggested that the bubble tip is located at a level that corresponds either to the liquid holdup in the liquid slug in front of the bubble, or to the critical film level, whichever is lower. Fagundes Netto et al. (1999) developed an analytical model for the back of the bubble, assuming hydraulic jump behavior, sometimes followed by a tail.

Dumitrescu (1943) obtained an analytical solution for the approximate shape of a bubble rising in a vertical tube. The calculated profile had a rounded nose and a bullet shape, as confirmed by photographs captured by Davies and Taylor (1950), which also found that for long bubbles, the perfectly spherical shape of the bubble nose is independent of the bubble length.

Barnea (1990) studied the effect of the bubble shape on pressure drop calculations in vertical slug flow. It was found that the assumption of a cylindrical Taylor bubble with a flat nose may yield incorrect results for pressure drop calculations, whereas taking into account the curved shape of the Taylor bubble's nose is essential for obtaining consistent results for the pressure drop.

Polonsky et al. (1999a) performed quantitative measurements of the Taylor bubble shape and of the liquid film thickness. The results were obtained by digital image processing of continuous sequences of video images and agree quite well with the model of Barnea (1990). It was found that the film thickness at the bubble nose increases with increasing liquid velocity; this effect vanishes far from the bubble nose. The experiments also showed that the bubble shape does not depend on the bubble length, in

* Corresponding author.
E-mail address: shemer@eng.tau.ac.il (L. Shemer).
[1] Present address: Deptartment of Civil and Environmental Engineering, Technion, Haifa, Israel.

http://dx.doi.org/10.1016/j.ijmultiphaseflow.2016.05.011
0301-9322/

agreement with findings of Davies and Taylor (1950). Polonsky et al. (1999a) reported on strong oscillations of the Taylor bubble bottom and analyzed the characteristics of those oscillations. They showed that the averaged bottom of the bubble has a concave shape that is essentially insensitive to liquid velocity and bubble length.

Van Hout et al. (2002) investigated the velocity field induced by a Taylor bubble rising in stagnant water using Particle Image Velocimetry (PIV). They determined the shape of the Taylor bubble, using the same procedure as in Polonsky et al. (1999a). The measured results are in agreement with Ahmad et al. (1998) and Polonsky et al. (1999b).

Gu et al. (2007) studied experimentally the shape of a single bubble in horizontal flow, using visual observation and conductance probes. They found that at low Froude numbers (based on the mixture velocity) the bubble nose was located at the top of the pipe. The nose moves towards the center of the pipe with increasing Froude number. The shape of the tail region depends on the bubble length and on the Froude number. Roitberg et al. (2008) determined experimentally the ensemble-averaged shapes of the elongated bubble nose, liquid film and bubble tail in downward inclined slug flow using a wire-mesh sensor. The data was used to reconstruct the 3D structure of ensemble-averaged bubbles.

Dos Reis and Goldstein (2005) applied a non-intrusive capacitance probe for measuring the elongated bubbles' profile and their mean velocity in horizontal air-water slug flows. Pipa et al. (2014) obtained images of elongated bubbles in horizontal slug flow for various liquid and gas velocities. A new scheme for image processing was applied to characterize the bubble shape. Matamoros et al. (2014) and de Oliveira et al. (2015) also used optical methods to investigate experimentally the shape of long bubbles in horizontal slug flow.

The present research is aimed at studying the effect of pipe inclination and of gas and liquid flow rates on the elongated bubble shape in continuous slug flow.

2. Experimental facility, measurement methods and data processing

Experiments with water and air as working fluids were carried out in a 10 m long pipe, open to atmosphere (Fig. 1). The pipe is supported by a steel frame and can be fixed by a hydraulic system at any angle of inclination β, from horizontal ($\beta = 0^o$) to vertical. The pipe is made of transparent Perspex and has an internal diameter of 0.054 m. The two fluids are introduced to the pipe simultaneously through a "mixer" type inlet device, which is 0.3 m long (Fig. 1). For a detailed description of the facility see van Hout et al. (2003) and Barnea et al. (2013). The measuring station is located at a distance of about 8 m from the inlet, sufficiently far from the inlet to insure flow development and appropriately far from the outlet of the pipe to eliminate end effects.

A wire mesh sensor supplied by Teletronic Rossendorf is used as the major device for the cross sectional phase distribution measurements (see Barnea et al. 2013). Conductance probes are used as a subsidiary instrument for the determination of the interface velocity.

The sensor consists of two parallel wire layers perpendicular to the pipe axis, the spacing between the layers is 2 mm. The operation principle of the wire mesh sensor is based on the difference in electrical conductivity of air and water. Each layer of the sensor is built of 16 parallel 0.125 mm steel wires with constant spacing of 3.3 mm. The schematic outline of the sensor is also presented in Fig. 1. The operation principle of the wire-mesh sensor is based on the difference in electrical conductivity of air and water. One layer is used as a receiver, while the other one as a transmitter. The wires in both layers form a rectangular mesh. Only 208 out of total 256 junctions in the mesh are located within the pipe cross section. Each wire in the transmitter plane is periodically activated using a multiplexer circuit by a short voltage pulse. An additional multiplexer circuit is used to connect consecutively each one of the receiver's wires during the single pulse supplied to the transmitter wire.

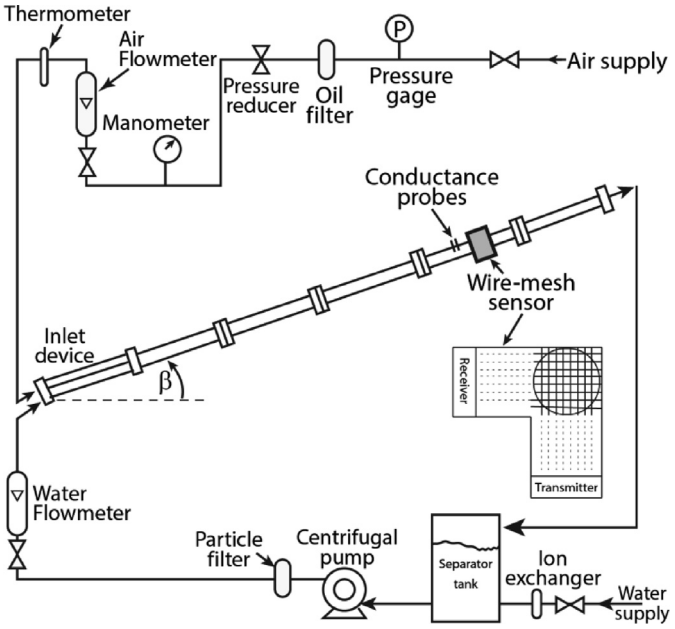

Fig. 1. Experimental facility layout.

The wire mesh sensor provides direct information on the cross-sectional instantaneous phase distribution and is free of inversion problems, common to other tomographic methods. The sensor introduces disturbances that may affect the spatial structure of the flow in its wake. These disturbances, however, mostly occur downstream of the sensor, so that the collected data are almost undisturbed by the instrument.

The resolution along the pipe axis is determined by the interface propagation velocity, as well as by the sampling frequency. The instrument is capable of sampling at frequencies up to 10 kHz for the whole cross section; in most cases, the maximum available sampling frequency was used. The wire-mesh sensor thus provides high-frequency data on the temporal variation of the local void fraction at each junction of the mesh. These temporal records can be translated into corresponding lengths, provided the elongated bubble's propagation velocity is known. The propagation velocities were measured using two conductance tip probes with axial separation of 5 cm that protruded by about 2 mm from the top of the pipe wall. A thin copper foil glued to the pipe bottom served as the common ground electrode. Positive DC voltage was supplied to the top probes. The voltage between each of the tip probes and the ground was sampled at a frequency of 10 kHz. The interface propagation velocity is obtained by determining the time delay between the maxima of cross-correlation coefficient of two probes' outputs.

The voltages recorded at each junction of the wire-mesh sensor are translated into the local instantaneous void fraction using the calibration coefficients determined before the beginning of each experimental run. The conductivity value of unity is prescribed to a junction fully immersed in water and zero to a junction surrounded by gas. In the course of the calibration procedure, the output voltages for each junction in the mesh are recorded, first for an empty pipe, and then for a pipe filled with water. Following Prasser et al. (1998), linear dependence is assumed between the output voltages and the instantaneous void fraction in the vicinity of the